Displacing difficult yield stress fluids from pipes

Ian A. Frigaard[1], Jaewoo Jeon[1], Gustavo Moises[2,3], Monica F. Naccache[3], and Kamran Alba[4]

[1] Mechanical Engineering, University of British Columbia, Vancouver, Canada
[2] Petrobras, Rio de Janeiro, Brazil
[3] Department of Mechanical Engineering, PUC-Rio, Rio de Janeiro, Rio de Janeiro 22451-900, Brazil
[4] University of Houston, Houston, TX, United States

ABSTRACT
Having yield stress fluids (YSFs) stuck in ducts is a common occurrence in industrial and natural settings that range from flow assurance in pipelines, through mucus-blocked aioli in pneumonia to the cleaning of dairy products in food processing. Here, we give an overview of recent experimental studies in which pipes filled with YSFs (Carbopol) are cleaned by displacing with a Newtonian fluid (water).

INTRODUCTION
Examples of processes in which it is necessary to remove a gelled material from a duct include oil & gas well cementing,[6] waxy crude oil pipeline restarts,[4] Enhanced Oil Recovery (EOR),[1] Gas Assisted Injection Molding (GAIM),[3] biomedical applications,[2] cleaning of equipment and stubborn soil,[7] food processing[5] and personal care.[8] A wide range of models are developed to describe residual deposits in these situations, ranging from viscoplastic yield stress descriptions through to elastic gels. Industrially, cleaning effectiveness is often measured in terms of a cleaning time,[5,12] which is observed to vary with the flow parameters. Others seek to understand cleaning indirectly via characterizing the observed flow behaviours,[8] and this is our approach in this paper.

We present a synopsis of our work over the past 5 years[9,11,13–15] in which we remove a yield stress fluid from a long pipe by displacing with a viscous fluid, largely pumped at laminar flow rates. As our work is motivated by oilfield cementing operations,[6] we consider different combinations of density to give both density-unstable and density-stable flows. The flows also take place over a wide range of pipe inclinations. In order to make our study tractable, in terms of the wide range of dimensionless groups that could be studied, we have focused our work on *difficult* displacements.

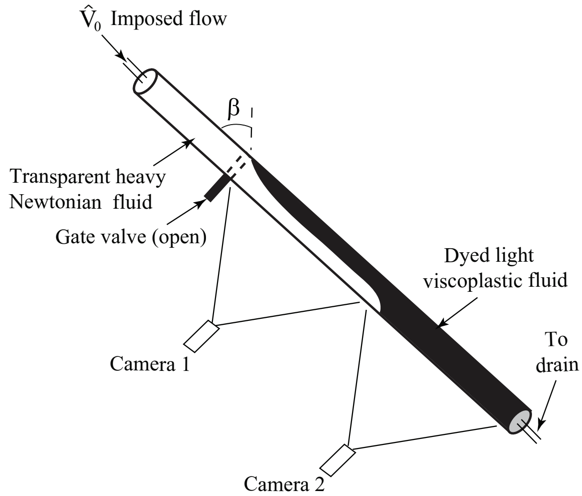

Figure 1. Schematic of the experimental setup used, for a density-unstable configuration

With the general setup of Fig. 1, *difficult* displacements satisfy the following constraints.

- The viscous stresses $\hat{\tau}_v$ are small relative to the yield stress $\hat{\tau}_Y$, i.e. $\hat{\mu}\hat{V}_0/\hat{D} = \hat{\tau}_v \ll \hat{\tau}_Y$, or alternately:

$$B_N \gg 1, \qquad B_N = \frac{\hat{\tau}_Y \hat{D}}{\hat{\mu}\hat{V}_0}. \tag{1}$$

Here B_N is a Bingham number, but with the viscous stress scale coming from the Newtonian fluid: $\hat{\mu}$ is the Newtonian fluid viscosity, $\hat{V}_0$ is the mean displacement velocity and $\hat{D}$ is the pipe diameter.

- We allow the inertial stresses $\hat{\tau}_t$ to be comparable to the yield stress, i.e.

$$\hat{\rho}\hat{V}_0^2 = \hat{\tau}_t \lesssim \hat{\tau}_Y, \qquad (2)$$

where $\hat{\rho} = (\hat{\rho}_H + \hat{\rho}_L)/2$ is the mean density of heavy and light fluids. We consider a range of $Re = \hat{\rho}\hat{V}_0\hat{D}/\hat{\mu} > 1$, but (2) also restricts $\hat{\tau}_t$ and is equivalent to $Re/B_N \lesssim 1$.

- We consider displacements flows in which buoyancy stresses $\hat{\tau}_b$ may be significant in affecting yielding:

$$|\Delta\hat{\rho}|\hat{g}\hat{D} = \hat{\tau}_b \lessapprox \hat{\tau}_Y, \qquad (3)$$

where $\Delta\hat{\rho}$ is the difference in density between the fluids and $\hat{g}$ is the gravitational acceleration.

The 3 conditions (1)-(3) define the parameter space of our experiments, reducing the relevant parameter space significantly from the 8 dimensionless parameters. Apart from the groups introduced above, the density difference is characterized by the dimensionless Atwood number ($At = (\hat{\rho}_H - \hat{\rho}_L)/(\hat{\rho}_H + \hat{\rho}_L)$), the ratio of inertial and buoyancy forces is characterized by the densimetric Froude number ($Fr = \hat{V}_0/(At\ \hat{g}\hat{D})^{1/2}$), and pipe inclination from vertical is β.

Although focusing on a subset of displacements is restrictive, it also allows an extensive study, and many 100's of experiments have been performed.[9,11,13–15] All of these experiments have used the same flow loop and very similar combination of fluids. the yield stress fluid is a Carbopol solution and the displacing fluid is water; either salt or glycerol used to adjust the density difference. The displaced fluid is characterised rheologically as a Herschel-Bulkley fluid and the displacing fluid is Newtonian. Approximately 20 different fluid pairings have been tested, with different imposed flow rates and different pipe inclinations.[9,11,13–15] A summary of the important dimensionless parameter ranges covered experimentally in these studies is provided in Fig. 2.

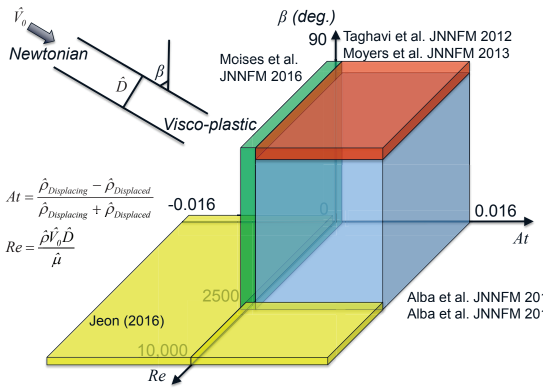

Figure 2. Overview of visco-plastic displacement studies

ISODENSE DISPLACEMENTS

Iso-dense displacements were studied extensively by Moises *et al.*[15] with recent extensions.[13] The main observations, over a range of 9 different fluid pairings, was that the flow type undergoes a significant transition as the displacement flow rate is increased. At low displacement rates the Newtonian fluid channels through the yield stress fluid, leaving behind an uneven rugous residual layer at the walls. On increasing the flow rate the rugosity decreases, but the layers remain static in the pipe with a more wavy variation. At higher flow rates the waviness vanishes and a smooth wall layer persists. Finally, at sufficiently large flow rates weakly turbulent mixing ensues, generally removing the wall layer (over the ranges studied). These 4 regimes have been termed *corrugated*, *wavy*, *smooth* and *mixed* regimes.

An example of the transition from corrugated to smooth regimes is illustrated in Fig. 3a and typical variations in the depth averaged fluid concentrations are shown in Fig. 3b. The variations in the concentration and corresponding variations in the front velocity have been used to give a combined measure of the uncertainty ($\delta Q/\bar{Q}$) in the experimental quality $\bar{Q}$. The uncertainty is defined[15] in such a way as to represent the deviation of the flow from a steadily propagating front of fixed shape.

Threshold values of the uncertainty are then used to quantitatively categorize the different flows types, as indicated in Fig. 4. It is also

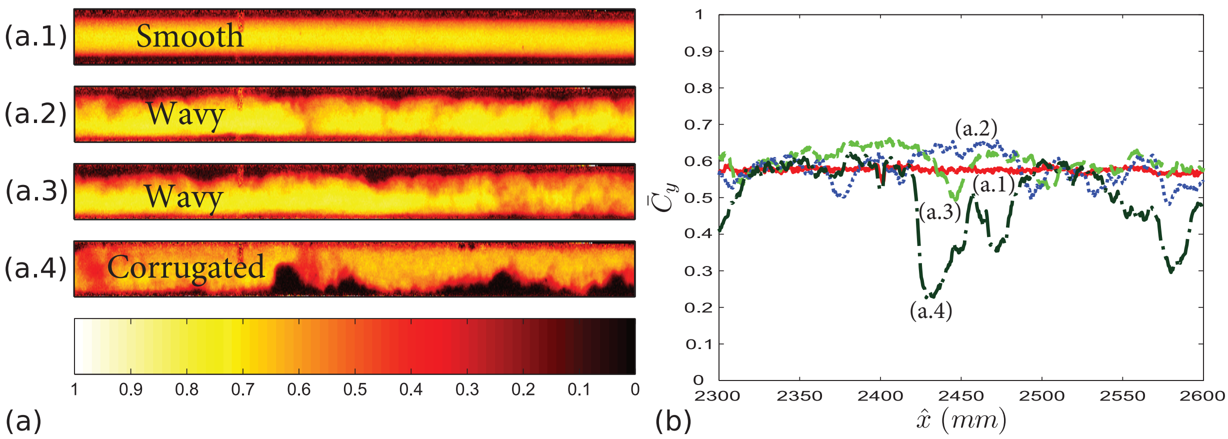

Figure 3. Transition from corrugated to smooth regimes.[15] a) Snapshots of the concentration field for a 385mm long section of the pipe, 2286mm downstream of the gate valve after the passage of the front: (a.1) $\hat{V}_0 = 47.4$mm/s; (a.2) $\hat{V}_0 = 20.7$mm/s; (a.3) $\hat{V}_0 = 14.3$mm/s; (a.4) $\hat{V}_0 = 4.4$mm/s. b) Depth-averaged concentration $\bar{C}_y$ values with streamwise distance, $\hat{x}$, for the same experiments: a.1 (solid line), a.2 (dotted line), a.3 (dashed line) and a.4 (dotted-dashed line).

found that the regimes may be delineated by threshold values of a Reynolds number Re_Y, that is based on on the effective viscosity of the displaced fluid:

$$Re_Y = \frac{8\hat{\rho}\hat{V}_0^2}{\hat{\tau}_Y + \hat{\kappa}\hat{\dot{\gamma}}_c^n} : \qquad \hat{\dot{\gamma}}_c = \frac{8\hat{V}_0(3n+1)}{4n\hat{D}}.$$

Here $\hat{\kappa}$ and n are the consistency and power law index of the displaced fluid.

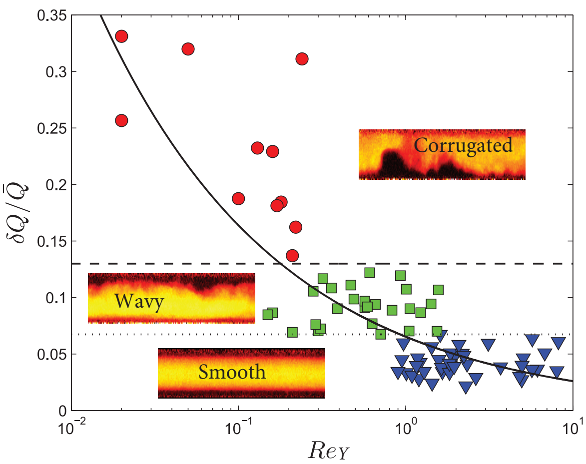

Figure 4. Classification of the flows of Moises *et al.*[15] using uncertainty $\delta Q/\bar{Q}$ or Re_Y. Red, green and blue symbols denote corrugated wavy and smooth symbols respectively.

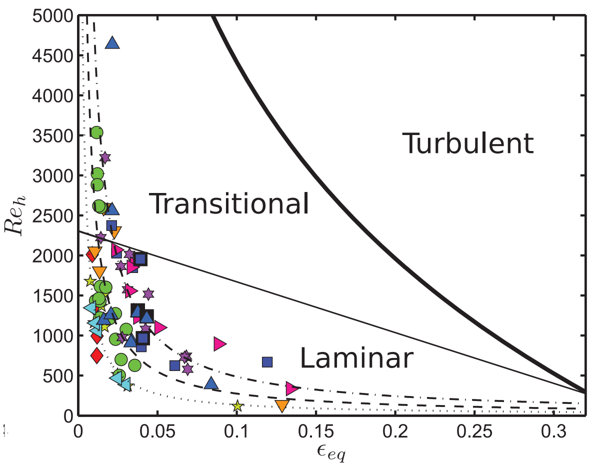

Figure 5. Overview of visco-plastic displacement studies: Flow dynamics classification of displacing fluid in the plane of hydraulic Reynolds number, Re_h, and interfacial roughness, ε_{eq}. $Re_L = -6340.3\varepsilon_{eq} + 2304.4$ (thin solid line), $Re_T = -3542\ln\varepsilon_{eq} - 3739.6$ (thick solid line), $Re_h = 13/\varepsilon_{eq}$ (- - -), $Re_h = 26/\varepsilon_{eq}$ (.-.-.-), $Re_h = 48/\varepsilon_{eq}$ (. . . .). Different markers represent experimental batches with various yield stresses.

It is evident that the restriction of the pipe, due to the residual layers on the wall, and the rugosity of the wall layer itself, may both affect the flow of displacing fluid. To investigate this we have used the variations in wall layer thickness to define a representative roughness of the wall layer, finding that it is typically outside the range of roughness considered in standard hydraulics closures. However, recent work[10] targets specifically pipe flows with "large roughness". Using these expressions[10] and developing a Reynolds number Re_h based on the hydraulic diameter and effective roughness of the displacing fluid flow cross-section, we are able to approximately classify the flow; see Fig. 5. The majority of the experiments are in laminar and transitional regimes (as the flow rate is increased and/or due to flow restriction/roughness), but few are classified as turbulent. More recently[13] the range was extended into the turbulent regime.

DENSITY-UNSTABLE DISPLACEMENTS

Density-unstable displacements (see Fig. 1) have been studied[9,11,13,14] extensively. Two main categories of displacement have been identified: *central* and *slump* types. The central type displacements tend to propagate as a finger along the centre of the pipe leaving behind residual wall layers, whereas the slump type displacements tend to propagate along one side of the pipe. In inclined pipes the heavier fluids tend to follow the lower wall. As the flow rate is increased sufficiently, both flow types transition to a *mixed/turbulent* regime.

Figure 6 shows a compilation of the existing data,[9,11,13,14] classified by regime and plotted in the $(Fr, Re/Fr)$-plane. The transition between central and slump-type displacements occurs in the range $Re/Fr = 600-800$. It is noted that

$$\frac{Re}{Fr} = \frac{\hat{\rho}_H([\hat{\rho}_H - \hat{\rho}_L]\hat{g}\hat{D}^3)^{1/2}}{[\hat{\rho}_H + \hat{\rho}_L]^{1/2}\hat{\mu}},$$

representing a buoyancy-viscosity balance, but curiously independent of $\hat{V}_0$ and β. In Fig. 6 the datasets correspond to experimental fluid pairs with fixed At and similar viscosities, so that $Re/Fr \approx$ constant in each experimental sequence. Although Fr is plotted on the horizontal axis, it equivalent to increasing Re in these sequences. The transition to mixed/turbulent appears to be an inertial turbulent transition, perhaps aided by buoyancy (as it occurs earlier at higher Re/Fr).

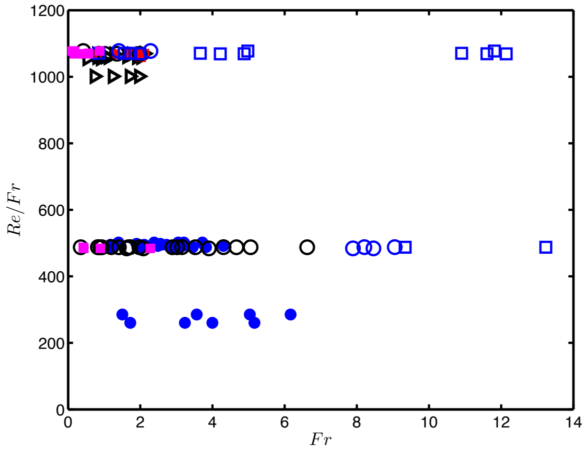

Figure 6. Density-unstable flows from Jeon (2016):[13] mixed/turbulent (□) central (○); slump (■), transitional (○). Experiments from Alba *et al.* (2013):[11] turbulent/mixed (■); slump (▷); central (●).

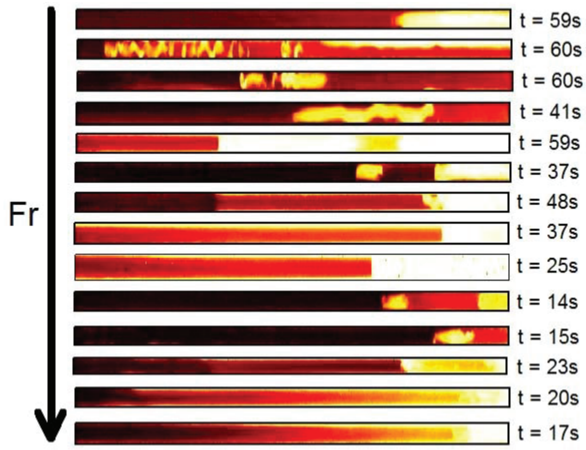

Figure 7. Images of vertical displacement flows[13] at $Re/Fr = 1100$. Times on right side of the images indicate the time after gate valve opening. Images are sequenced in order of increasing Fr.

Figure 7 shows images from different experiments in a vertical pipe,[13] performed at $Re/Fr = 1100$. We observe a range of symmetric and asymmetric regimes. Thus, although the slump-central classification seems remarkably independent of β, with no pipe inclination the classification fails. This suggests that the primary role of the unstable density difference is to allow different propagation modes to emerge than the axisymmetric, with β having a diminishing secondary role in flow selection as $\beta \to 0$.

The central regimes are qualitatively similar to the isodense displacement described in the previous section: the wall layers are uneven to varying degrees and are static, the displacing fluids are Newtonian and generally in laminar flow; see Fig. 8a for an example velocity profile.

The range of flows encountered in the slump regime is very broad. A general trend is for a fast moving front to penetrate along one wall. Periodically this fast moving front may tend to rupture through the thick displaced fluid layer above, before again propagating further along the lower side. These have been termed *ripped* displacements. In cases where this process breaks the layer of displaced fluid, we sometimes observe a backflow of the lighter displaced fluid, propagating upwards against the flow. The upper layer of displaced fluid may either be static or mobile, generally with a plug-like axial velocity. The displacing fluid in the lower layer is accelerated by the constricted cross-section, which may result in high laminar-transitional-low turbulent velocities. Examples of velocity profiles illustrating these possibilities in both layers are shown in Fig. 8b & c. At high flow rates, fully mixed flows results as illustrated in Fig. 8d, with velocity profiles that appear weakly turbulent.

The dynamics of the displacing fluid layer have been analyzed further[14] in two directions. Firstly, we have analyzed the roughness of the displacing layer boundary and computed corresponding hydraulic Reynolds numbers, from which we are able to classify[10] the different flow regimes; see Fig. 9. Broadly similar results are found by Jeon,[13] with some flows extending into larger interfacial roughness values.

Secondly, the friction factor approximations developed have been used to estimate the

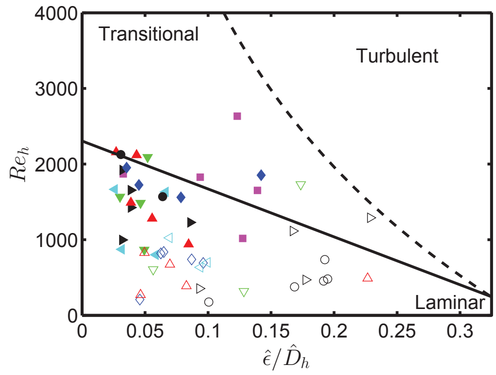

Figure 9. Dynamics of the displacing fluid layer classified[10] in terms of *laminar*, *transitional* and *fully rough* (turbulent) in the plane of Re_h and $\hat{\varepsilon}/\hat{D}_h$. Different markers represent $\beta = 0°$ (□), 15° (▷), 30° (◇), 45° (△), 60° (▽), 75° (◁) and 85° (○). Solid and hollow symbols refer to center-type ($At = 0.0035$) and slump-type flows ($At = 0.016$) respectively.

wall shear stress in these flows, (scaled with the yield stress); see Fig. 10. This reveals that the wall shear stresses generated during central type displacements are far below the yield stress of the fluid (confirming that the wall layers remain static). For slump type flows the accelerated displacement layer does generate wall shear stresses that are comparable with the displaced fluid yield stress. Note that in addition extensional stresses will result near the tip, from the mobile downstream flow. This *weakening* of the gel is likely to be the mechanism that allows rupturing of the in situ fluid.

DENSITY-STABLE DISPLACEMENTS

Density-stable displacements are less relevant to primary cementing downwards displacement flows and accordingly the range of flows studied is reduced, limited only to vertical pipes.[13] The effect of having a density-stable displacement is to increase the wall shear in the displaced fluid,[13] as can be easily demonstrated in simple axisymmetric multi-layer models and can be estimated from calculated friction fac-

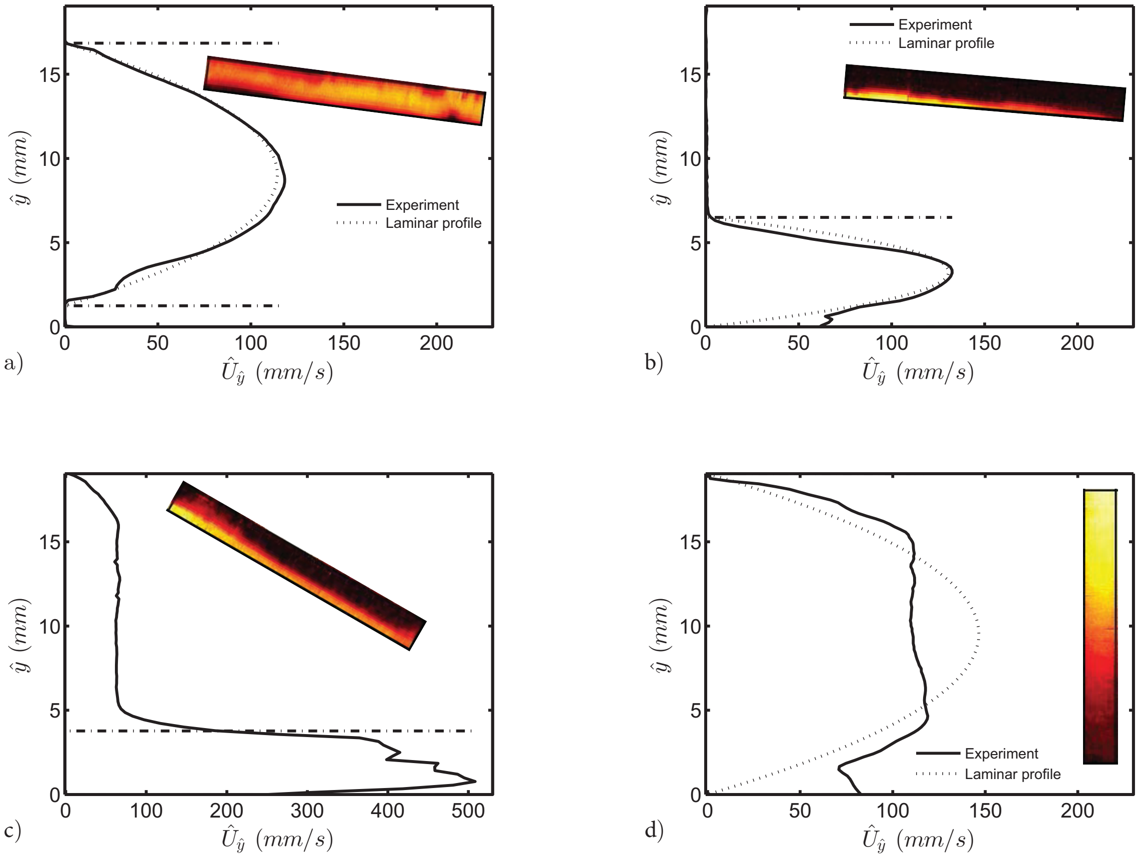

Figure 8. Example Ultrasonic Doppler Velocimetry (UDV) profiles and snapshots for different fluid pairings:[14] a) $\beta = 83°$, $At = 0.0035$, $\hat{V}_0 = 71$ mm/s; b) $\beta = 85°$, $At = 0.016$, $\hat{V}_0 = 30$ mm/s; c) $\beta = 60°$, $At = 0.016$, $\hat{V}_0 = 89.58$ mm/s; d) $\beta = 0°$, $At = 0.016$, $\hat{V}_0 = 97.66$ mm/s.

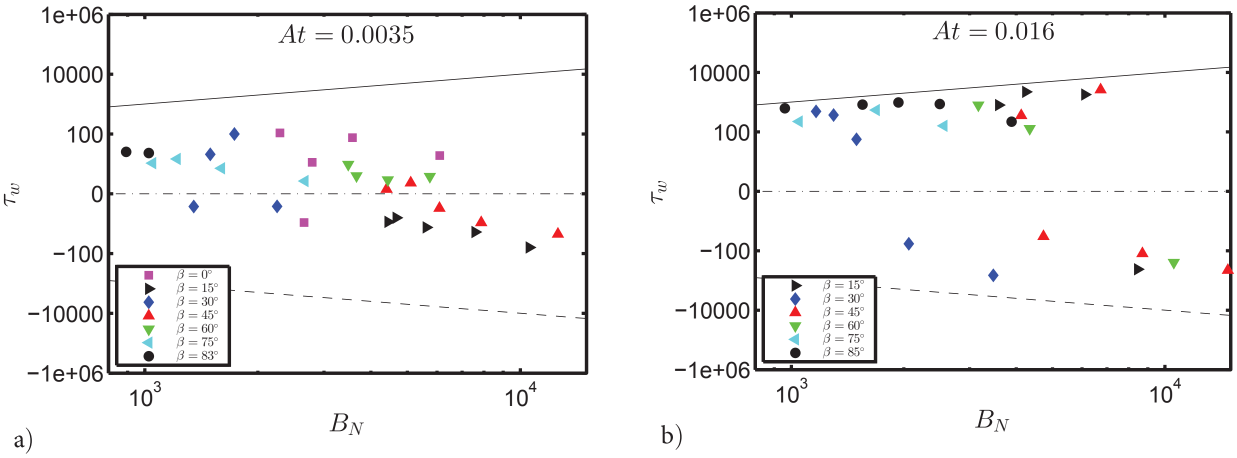

Figure 10. Dimensionless wall shear stress, τ_w, calculated[14] for center-type flows (left) and slump-type flows (right). The solid and dashed lines indicate $\tau_w = \pm B_N$.

tors, accounting for the residual wall layers and roughness. Thus in general, static residual wall layers are reduced and displacements are more efficient.

Visually, we see different types of displacement flow. These are largely central flows. Firstly, we have some flows that have a flat/blunt finger-like profile and leave behind static wall layers. Secondly, we have some flows in which the displacing fluid disperses ahead into the displaced fluid, moving centrally; see Fig. 11. Thirdly, we have flows that show some form of viscous fingering, which may co-exist with a second slower front. In the viscous fingering, an initial finger propagated ahead through the displaced fluid, either at the pipe centre or at the wall (and sometimes switching position downstream). The finger invariably destabilizes, often leading to helical patterns; see Fig. 12. Finally, at higher flow rates the dispersive flows become progressively unsteady, often leading to increasingly effective transverse mixing: a diffusive turbulent/mixing regime results; see Fig. 13. From the perspective of the wall layers, we have either efficient displacement, or stationary layers or layers that are effectively eroded via local mixing at higher flow rates.

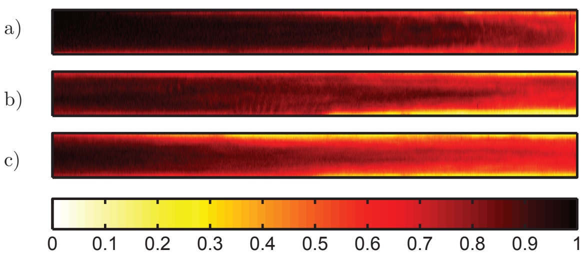

Figure 11. Flat central flow with $\hat{\tau}_y$ = 6.51 Pa, At = -0.0035: (a) $\hat{V}_0$ = 11.7 mm/s, $\hat{t}$ = 97s after the opening the gate valve. (b) $\hat{V}_0$ = 19 mm/s, $\hat{t}$ = 106s after the opening the gate valve. (c) $\hat{V}_0$ = 102 mm/s, $\hat{t}$ = 18.25s after the opening the gate valve.

CONCLUSIONS

We have given an overview of recent studies on displacement flow of a viscoplastic fluid by a Newtonian fluid along a pipe, covering broad variations in fluids properties, inclination angles and imposed flow rates. The flows have been categorized into three major configurations namely iso-dense, density-unstable and density-stable. Depending on the governing parameters, a wide range of flows appear, namely: central, slump, ripped, mixed, finger-type etc., all exhibiting varying ranges of flow instability and residual layer thickness/variation.

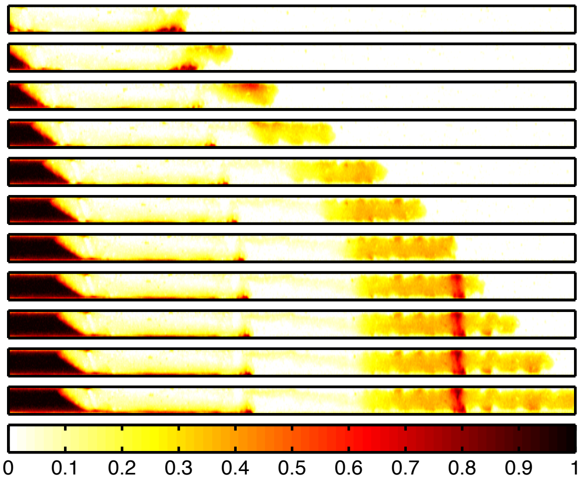

Figure 12. Viscous fingering in the density-stable displacement flow with $\hat{\tau}_y$ = 20.165 Pa, At = -0.016, $\hat{V}_0$ = 11.5 mm/s. The side view image of the displacement at $\hat{t}$ = 92, 95 ... 119, 122 s after opening the gate valve. The images are taken 2315 mm below the gate valve. The size of the images are 19 $\times$ 675 mm^2.

ACKNOWLEDGEMENTS

We thank the following organizations for funding that has contributed to this research: NSERC, Schlumberger, BC Oil and Gas Commission, Petrobras S.A. and Brazilian funding agencies (MCTI/CNPq, CAPES, FAPERJ and FINEP).

REFERENCES

1. Lake, L. (1989), “Enhanced oil recovery”, Prentice Hall.

2. Howell, P., Waters, S. and Grotberg, J. (2000), “The propagation of a liquid bolus along a liquid-lined flexible tube”, *J. Fluid Mech.*, **406**, 309–335.

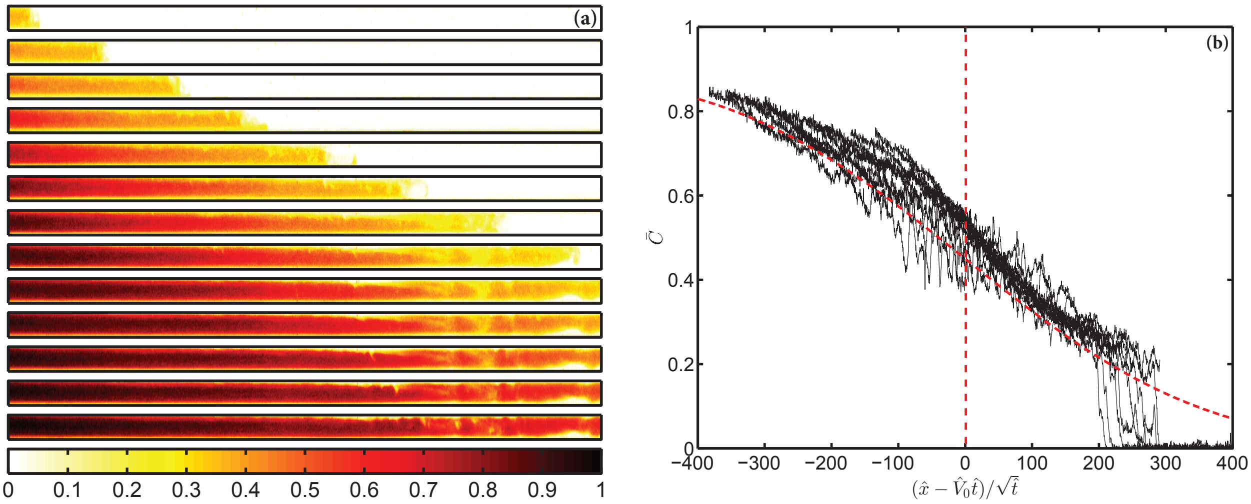

Figure 13. Turbulent/mixed regime in the density-stable displacement flow with At = -0.0035, $\hat{\tau}_y$ = 1.17 Pa, Re_N = 3744: (a) Side view images of the displacement at $\hat{t}$ = 5.25, 5.75 ... 9.75, 10.25 s after opening gate valve. (b) Collapse of the depth averaged concentration profiles plotted against $(\hat{x}-\hat{V}_0\hat{t})/\sqrt{\hat{t}}$. Red dash line indicates $\bar{C}$ = 1/2 erfc $\left((\hat{x}-\hat{V}_0\hat{t})/(2\sqrt{\hat{D}_M\hat{t}})\right)$ with $\hat{D}_M$ = 4 x $10^{-2}m^2/s$.

3. Parvez, M., Ong, N., Lam, Y. and Tor, S. (2002), "Gas-assisted injection molding: the effects of process variables and gas channel geometry", *J. Mat. Process. Tech.*, **121**, 27–35.

4. Vinay, G.2005"Modélisation du redemarrage des écoulements de bruts parafiniques dans les conduites pétrolieres".

5. Fryer, P., Christian, G. and Liu, W. (2006), "How hygiene happens: physics and chemistry of cleaning", *Int. J. Dairy Technol.*, **59**, 76–84.

6. Nelson, E. and Guillot, D. (2006), "Well Cementing, 2nd Edition", Schlumberger Educational Services.

7. Burfoot, D., Middleton, K. and Holah, J. (2009), "Removal of biofilms and stubborn soil by pressure washing", *Trends Food Sci. Tech.*, **20**, S45–S47.

8. Cole, P., Asteriadou, K., Robbins, P., Owen, E., Montague, G. and Fryer, P. (2010), "Comparison of cleaning of toothpaste from surfaces and pilot scale pipework", *Food Bioprod. Process.*, **88**, 392–400.

9. Taghavi, S., Alba, K., Moyers-Gonzalez, M. and Frigaard, I. (2012), "Incomplete fluid-fluid displacement of yield stress fluids in near-horizontal pipes: experiments and theory", *J. non-Newt. Fluid Mech.*, **167-168**, 59–74.

10. Huang, K., Wan, J., Chen, C., Li, Y., Mao, D. and Zhang, M. (2013), "Experimental investigation on friction factor in pipes with large roughness", *Exp. Therm. Fluid Sci.*, **50**, 147–153.

11. Alba, K., Taghavi, S., Bruyn, J. and Frigaard, I. (2013), "Incomplete fluid–fluid displacement of yield-stress fluids. Part 2: Highly inclined pipes", *J. Non-Newt. Fluid Mech.*, **201**, 80–93.

12. Palabiyik, I., Olunloyo, B., Fryer, P. and Robbins, P. (2014), "Flow regimes in the emptying of pipes filled with a Herschel–Bulkley fluid", *Chem. Eng. Res. Des.*, **92**, 2201–2212.

13. Jeon, J.2016"Displacing Visco-Plastic fluid with Newtonian fluid in a vertical circular pipe with various density combinations".

14. Alba, K. and Frigaard, I. (2016), "Dynamics of theremoval of viscoplastic fluids from inclined pipes", *J. Non-Newt. Fluid Mech.*, **229**, 43–58.

15. Moises, G., Naccache, M., Alba, K. and Frigaard, I. (2016), "Isodense displacement flow of viscoplastic fluids along a pipe", *J. Non-Newt. Fluid Mech.*, **236**, 91–103.